Chapter 5

The Paleocene-Eocene thermal maximum super greenhouse: biotic and geochemical signatures, age models and mechanisms of climate change

The geologically brief episode of global warming which occurred close to the Paleocene – Eocene boundary, termed the Paleocene – Eocene thermal maximum (PETM), has been extensively studied since its discovery in 1991. The PETM is characterized by a geographically quasi-uniform 5-8°C warming of Earth's surface as well as the deep ocean, and large changes in ocean chemistry. There is general consensus that the PETM was associated with the geologically rapid input of large amounts of CO_2 and/or CH_4 into the exogenic (ocean-atmosphere) carbon pool, but the source of this carbon is still under discussion. The biotic response on land and in the oceans included radiations, extinctions and migrations, and was heterogeneous in nature and severity. Debate continues on the total duration of the PETM, as well as on the relative amount of time involved in its onset, its relatively stable middle part, and its recovery phase. Recently, several events that appear similar to the PETM in nature, but of smaller magnitude, were identified in the late Paleocene through early Eocene, of which the timing was possibly modulated by orbital forcing. If these events and their astronomical pacing are confirmed, the trigger was probably insolation forced, excluding unique events as the cause of the PETM.

Close to the boundary between the Paleocene and Eocene epochs, approximately 55.5 Ma ago (Berggren et al., 1992; Chapter 2), a distinct phase of global warming occurred, which has been called the Paleocene-Eocene thermal maximum (PETM), and which was superimposed on already warm conditions. Evidence for the warming is seen inthe organic surface ocean paleothermometer TEX_{86}' (Chapters 3 and 4), negative oxygen isotope ($\delta^{18}O$) excursions in marine (Fig. 1) (Kennett and Stott, 1991; Thomas et al., 2002) and positive excursions in terrestrial carbonates (Koch et al., 1995), increased Mg/Ca ratios in planktic and benthic foraminifera (Zachos et al., 2003; Tripati and Elderfield, 2005), poleward migrations of (sub)tropical marine plankton (Kelly et al., 1996; Crouch et al., 2001) and terrestrial plant species (Wing et al., 2005), and mammal migrations across high northern latitudes (Bowen et al., 2002). Associated with the warming is a negative 2.5-6‰ carbon isotope ($\delta^{13}C$) excursion (CIE) (Kennett and Stott, 1991; Koch et al., 1992; Thomas et al., 2002; Pagani et al., 2006), generally accepted to reflect the geologically rapid injection of ^{13}C-depleted carbon, in the form of CO_2 and/or CH_4, into the global exogenic carbon pool (Fig. 1).

The apparent conjunction between carbon input and warming has fueled the hypothesis that increased CO_2 and/or CH_4 concentrations resulted in an enhanced greenhouse effect. The duration of the PETM, as defined by the negative carbon isotope excursion and subsequent recovery is still debated (Röhl et al., 2000; Bowen et al., 2001; Farley and Eltgroth, 2003; Röhl et al., in prep). The absolute amount of carbon input during the PETM (Dickens et al., 1997; Pagani et al., 2006; Chapter 1) might have been about 4-8 times the anthropogenic carbon release from the start of the industrial era up to today (Marland et al., 2005), and is comparable to that expected from anthropogenic emissions in the past and next centuries (IPCC, 2001). The PETM stands out in the fossil record as a time of major extinctions and radiations. In the past decade, a large number of papers have been generated on the PETM (Fig. 2), which are in general highly multi-disciplinary but sometimes predominantly aimed on specialists in the various fields. Here, we present a review on the present status of PETM research.

The age of the PETM

Initially, the PETM was placed within the latest Paleocene because it occurred before the biostratigraphic datum levels used to define the Paleocene-Eocene boundary (Berggren et al., 1995) therefore named the Late Paleocene thermal maximum (Zachos et al., 1993; see papers in Knox et al., 1996; and in Aubry et al., 1998). In 2000, the Paleocene – Eocene (P/E) boundary global stratotype section and point (GSSP) was formally defined at the base of the clay layer in the Gabal Dababiya section (Egypt). This level coincides with the steepest slope of the negative CIE (Aubry and Ouda, 2003; Gradstein et al., 2004) at this site. Hence, the P/E boundary can now be globally correlated based on recognition of the CIE, and the LPTM has been re-named the PETM. Some authors use the

term Initial Eocene thermal maximum (IETM), because the maximum absolute temperatures occurred after the Paleocene – Eocene boundary. We prefer the term PETM and use this throughout the paper. Considering the uncertainties in radiometric dating and orbital tuning, the PETM occurred in between 55.8 and 55.0 Ma ago (Berggren et al., 1992; Chapter 2).

In the marine realm, the PETM is located within planktonic foraminiferal zone P5 (Berggren et al., 1995), calcareous nannoplankton zone NP9 (Martini, 1971) and CP8 (Okada and Bukry, 1980), and its base occurs close to the benthic foraminiferal extinction (BFE) event (Fig. 1). In the North Sea, the CIE and its recovery cover the dinoflagellate cyst (dinocyst) zone *Apectodinium augustum* (Powell et al., 1996; Chapter 3). In the terrestrial realm, the base of the CIE coincides with the Clarkforkian - Wasatchian North American Land Mammal Age (NALMA) zone boundary, and is correlative or nearly so (within 10's to 100's of kyr) with the Gashatan – Bumbanian land mammal age boundary in Asia.

The carbon isotope excursion

Shape

The most consistent geochemical signature recorded about coeval with the PETM is the negative CIE (Fig. 1). Accurate knowledge of the true 'shape' of the CIE with respect to time would improve our ability to use $\delta^{13}C$ curves as a tool for correlation of PETM sections. The CIE is considered to reflect the injection of huge amounts of ^{13}C-depleted carbon into the ocean-atmosphere system, and its shape and magnitude are critical in elucidating the carbon source and the quantity of carbon input, as well as the mechanisms involved in the subsequent removal of the excess carbon (Dickens et al., 1997; Dickens, 2001a). Understanding the pattern of coupled, secular changes in the $\delta^{13}C$ of the oceans and atmosphere with time is therefore a prerequisite to interpreting the mechanisms enacting carbon cycle change during the PETM (Dickens, 2001a).

In marine deposits the CIE is typically characterized by a transient ~2.5 negative $\delta^{13}C$ step on average in benthic foraminifers, and a 2.5-4‰ negative step in planktonic foraminifers, followed by a relatively stable phase of low values – the body of the CIE - and a subsequent exponential recovery (Fig. 1). The asymmetric shape has been interpreted as a geologically rapid input of ^{13}C-depleted carbon into the system, followed by a gradual sequestration of the excess carbon. In general, post CIE $\delta^{13}C$ values appear always lower than pre-CIE values, which may be related to the background late Paleocene – early Eocene decrease in exogenic $\delta^{13}C$ (Zachos et al., 2001). Bulk carbonate $\delta^{13}C$ records locally show two negative steps at the onset of the PETM (Bains et al., 1999; Chapter 1) (Fig. 1), which has been interpreted as evidence for multiple injections of carbon (Bains et al., 1999). At Ocean Drilling Program (ODP) Site 690, the intermediate

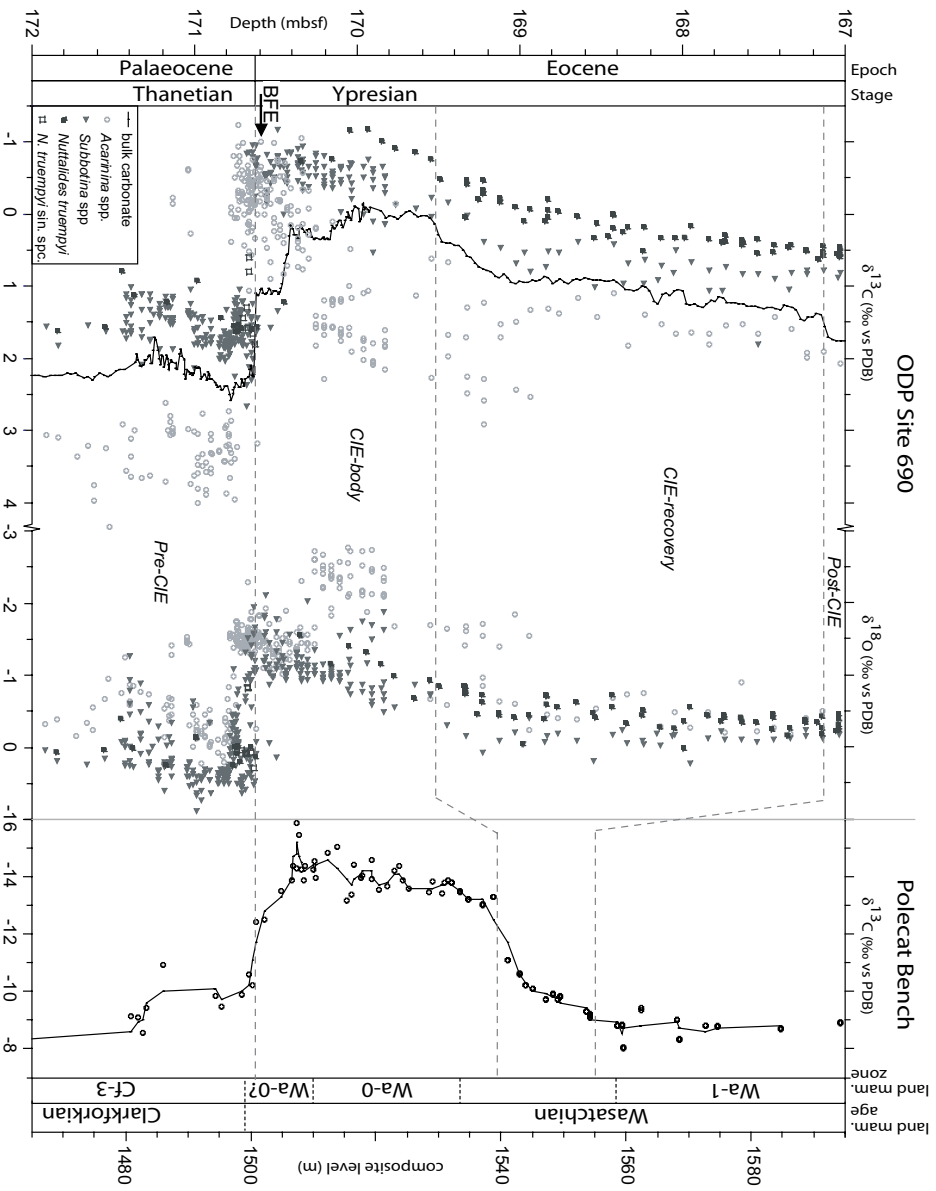

Figure 1. Compilation of $\delta^{13}C$ and $\delta^{18}O$ values of planktonic foraminifera (surface dweller Acarinina and thermocline dweller Subbotina spp.; mostly single specimen), benthic foraminifera (Nuttalides truempyi) and bulk carbonate from ODP Site 690 in the Weddel Sea (data from Kennett and Stott, 1991; Bains et al., 1999; Thomas et al., 2002; Kelly et al., 2005) and the soil carbonate nodule $d^{13}C$ record of Bowen et al., (2001) from the Polecat Bench section in the Bighorn Basin, Wyoming, USA. BFE refers to the main phase of benthic foraminifer extinction according to (Thomas, 2003).

$\delta^{13}C$ values that comprise the plateau were reproduced in the fine (3-5μm) size fraction of the sediment, dominated by the calcareous nannofossil species *Toweius* (Stoll, 2005). Further, it was reproduced in the 8-12μm size fraction, but this record was influenced by significant nannofossil assemblage shifts, which occurred concomitantly with the $\delta^{13}C$ steps (Bralower, 2002; Stoll, 2005). In the terrestrial realm, soil carbonate nodule $\delta^{13}C$ records from paleosol sequences in the Bighorn Basin, Wyoming, United States, show a 5-6‰ negative step at the onset of the PETM (Koch et al., 1992; Bowen et al., 2001). The general shape of the CIE is comparable to that of the bulk marine records, apparently including a short plateau during the onset of the CIE (Fig. 1). The general shape, sometimes including intermediate values, has been reproduced in several marine bulk carbonate and terrestrial soil nodule $\delta^{13}C$ (Fig. 1). Hence, many authors have used the inflection points in the ODP Site 690 bulk carbonate $\delta^{13}C$ record to correlate carbon isotope records generated in other basins, thereby assuming this record reflects the true $\delta^{13}C$ evolution of the exogenic carbon pool.

However, marine $\delta^{13}C$ records in general are influenced by dissolution and local productivity effects, which are likely associated with the different shapes and magnitudes of the CIE between the various planktonic microfossil records. Moreover, the intermediate plateau and several pronounced inflection points in bulk $\delta^{13}C$ records have not been reproduced in single foraminifer $\delta^{13}C$ analyses

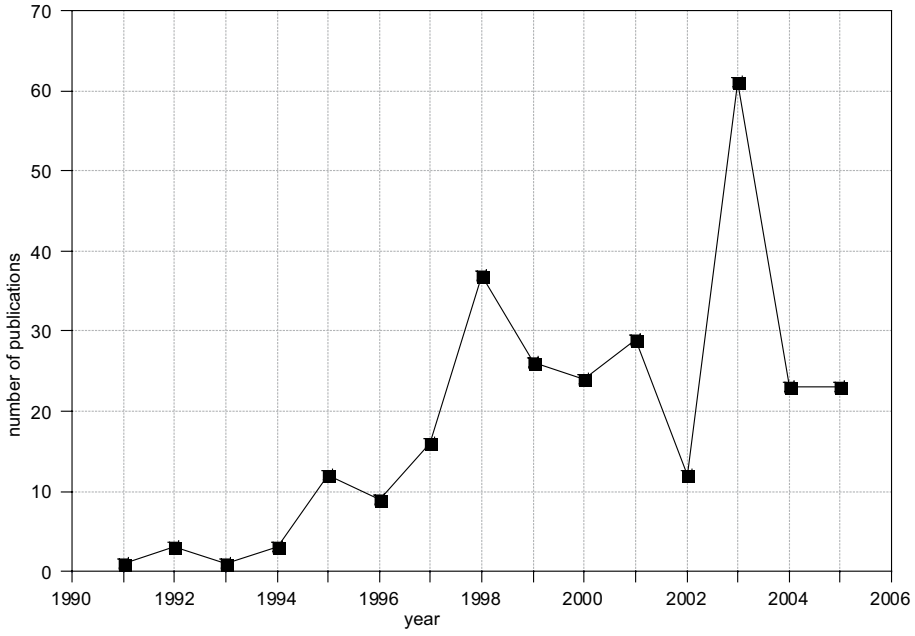

Figure 2. Number of studies focused published per year on the PETM since the first publication on its CIE and warming in 1991. Numbers are based on a Web of Science search using the keywords Paleocene, Paleocene, and Eocene.

(Fig. 1). This seriously questions the multiple injection hypothesis. Furthermore, along with potential dissolution and productivity effects laying at the root of the inflection points, it also questions if the Site 690 bulk carbonate $\delta^{13}C$ record reflects the $\delta^{13}C$ evolution of the global exogenic carbon pool through the PETM.

A puzzling aspect is the exact position of the onset of the CIE at Site 690. This position varies stratigraphically between the type of foraminifer species measured and/or the size fraction (Fig. 1; see also discussion of that problem in Thomas, 2003). These discrepancies have been extensively discussed (e.g., Thomas et al., 2002; Stoll, 2005) and it has been hypothesized that they reflect the propagation of the injected carbon and higher temperatures through the water column, local conditions (such as productivity changes) and/or post-depositional mechanisms (such as diagenesis and differential biototurbation; (Thomas, 2003). Above uncertainties hamper solid estimates of the time involved between the onset of the CIE and the minimum $\delta^{13}C$ values, which is important in estimating fluxes of carbon input (Dickens et al., 1997; Schmidt and Schindell, 2003) and thereby excluding hypothesized sources of the carbon.

The stratigraphic thickness of the recovery phase relative to the body of the event is larger in the marine records than in the terrestrial realm. This can be explained, at least in part, by strong variations in deep marine sedimentation rates due to the fluctuations in the depths of the lysocline and CCD (Chapter 1). Because there is no general consensus on the magnitude of the variations in sedimentation rates, particularly for the recovery phase (Röhl et al., 2000; Farley and Eltgroth, 2003; see below), the marine age models are not consistent. This is unfortunate because knowledge of the true shape of the PETM $\delta^{13}C$ curve is vital in correlating the marine to the terrestrial records and in assessing the $\delta^{13}C$ evolution of the exogenic carbon pool through time.

Magnitude

Large discrepancies in the absolute magnitude of the CIE exist between the records derived from the deep sea, the planktonic realm and the continents. Planktonic foraminifera show a 2.5-4‰ excursion (up to 4‰ in the mixed layer dweller *Acarinina*, 2-3‰ in the mixed layer dweller *Morozovella* and 2‰ in thermocline dweller *Subbotina* (e.g., Thomas and Shackleton, 1996; Thomas et al., 2002; Zachos et al., 2003; Tripati and Elderfield, 2004), while only a ~2‰ CIE is recorded in isolated calcareous nannofossils at Site 690 (Stoll, 2005). Although the average magnitude of the CIE measured on benthic foraminifera is ~2.5‰ (e.g., Kennett and Stott, 1991; Zachos et al., 2001; Nunes and Norris, 2006) (Fig. 1), considerable variation is observed between various benthic foraminifer $\delta^{13}C$ records. Nunes and Norris (2006) suggested that this reflects changes in oceanic circulation. However the benthic isotope records comprize mostly multi-specimen records which are likely influenced by bioturbation and therefore mixing between

pre-CIE and CIE specimens. Furthermore, some sites have suffered severe dissolution, while at other sites only very small benthics are present at the minimum $\delta^{13}C$ intervals implying that the records are incomplete. The CIE in soil carbonate nodules is 5-6‰ (Koch et al., 1992; Bowen et al., 2001; Bowen et al., 2002; Bowen et al., 2004), while it is 4-5‰ in terrestrial higher plant n-alkanes (Pagani et al., 2006). Although the magnitude among the many total organic carbon $\delta^{13}C$ records generated in terrestrial (Magioncalda et al., 2004) and marine (e.g., Dupuis et al., 2003; Steurbaut et al., 2003; Chapter 7) appears consistent at ~5‰, such records are likely influenced by changes in the source of the organic matter. In theory, the magnitude of the CIE should be the same in all reservoirs in the global exogenic carbon pool, as these should be in isotopic equilibrium over timescales such as the duration of the CIE. Hence, the variation in the magnitude of the CIE should, along with diagenetic issues, be assigned to changes in the habitat - which may particularly be the case for pelagic organisms – or changes in productivity, oceanic circulation or the fractionation of carbon isotopes.

Foraminiferal calcite becomes ^{13}C-enriched with lower pH and $[CO_3^{2-}]$ (Spero et al., 1997), which may explain a ~0.5‰ damping CIE in foraminifera (Bowen et al., 2004). Other factors that may potentially have contributed to at least a damped bulk marine CIE are changes in growth rate and cell size and geometry (e.g., Popp et al., 1998), which are likely to have occurred with the environmental change recorded at the PETM. Bowen et al. (2004) indicate that soil nodule $\delta^{13}C$ depends on the fractionation of the plants that grow on the soil. They conclude that the magnitude of the terrestrial CIE in the mid-latitudes relative to the marine CIE should be ascribed to increased fractionation of plants due to an increase of relative humidity and soil moisture. However, compound specific organic molecules (C29 n-alkanes) derived from terrestrial higher plant leaf waxes from the Arctic realm, where an increase in relative humidity is unlikely to have occurred at the PETM, also indicate a 4.5-5‰ CIE (Pagani et al., 2006). This value is close to the planktonic foraminifer CIE at Site 690, and may well reflect the actual magnitude of the atmospheric CIE.

Duration and age models

Age models for the PETM and CIE are in general agreement that the PETM was a geologically brief event (between 100 and 250 kyr in length), but different approaches have produced large differences in estimates of the total duration and the duration of different parts (Fig. 1) of the event. In part, these differences may be explained by uncertainties in the exact definition of the CIE itself. The onset is usually easily identified at an abrupt negative step (which, however, not always occurs at the same level in foraminifer and bulk isotope data (Fig. 1) and in terrestrial soil nodule and dispersed organic carbon, Magioncalda et al., 2004), but the termination of the CIE somewhat subjective because it is exponential (Fig. 1). Here, we will discuss and update previously published age models.

Work on the Polecat Bench section in the Big Horn Basin in Wyoming has produced an estimate for the duration of the PETM in the terrestrial realm, based on the stratigraphic thickness of the CIE and average sedimentation rates during Magnetochron C24r, using the 2.557myr estimate of Cande and Kent (Cande and Kent, 1995) for the duration of C24r. Sedimentation rates in that basin depend largely on the accommodation space resulting from presumably constant subsidence. Bowen et al. (2001) show a ~40m stratigraphic thickness for the body of the CIE (Fig. 1). The thickness of the recovery is ~15m, resulting in a ~55m thickness for the CIE. Average sedimentation rates of 47.5cm per kyr for Chron C24r were calculated from the age-model presented by Gingerich (2000), which is based on the magnetostratigraphy of Butler et al. (1981). Hence, Bowen et al. (2001) imply a ~84kyr duration for the body of the CIE (Fig. 1). More recently, Koch et al. (2003) updated the magnetostratigraphy and showed that ~1030m of sediment accumulated during C24r, which would result in average sedimentation rates of 40.2cm.kyr^{-1}, implying a ~71kyr duration for the body of the CIE.

However, recent studies on astronomically-derived cycles from complete earliest Paleogene successions from ODP Leg 208 on the Walvis Ridge have revealed that much more time is represented in the interval between the CIE and the Chron 24r/24n reversal (Chapter 2) than estimated by Cande and Kent (Cande and Kent, 1995). The whole duration of Chron 24r was in the order of 3.118myr (Westerhold et al., submitted). This implies that average sedimentation rates in the basin during C24r were approximately 33.0cm.kyr^{-1} (i.e., 1030m/3.118myr), significantly lower than previous estimates, resulting in an estimate of the duration of the body of the CIE of ~120kyr (i.e., 40m/33.0cm.kyr^{-1}) and ~170kyr (i.e., 55m/33.0cm.kyr^{-1}) for the whole PETM.

Two age models are derived from the PETM section at ODP Site 690 on Maud Rise in the Weddel Sea, which is relatively expanded for deep marine deposits. Röhl et al. (2000) presented Fe and Ca records from core-scan X-Ray Fluorescence (XRF) measurements through the CIE. Identification of onset of the recovery and the termination of the CIE are problematic (Fig. 1), but they counted 4 precession-related cycles within the body of the CIE, 11 cycles within the entire CIE based on inflection points of the bulk carbonate $\delta^{13}C$ record. They attribute these cycles to climatic precession and, hence, arrived at an estimate for the entire CIE of 210 to 220kyr.

Farley and Eltgroth (Farley and Eltgroth, 2003) argued that Site 690, like many deep marine sites experienced rapid sedimentological changes during the PETM and question precession as a forcer for the cycles that Röhl et al. (2000) recognized. To build an independent age model, Farley and Eltgroth determined the extraterrestrial ^3He ($^3He_{ET}$) concentrations of Site 690 and assumed that the extraterrestrial flux of this isotope to the Earth remained constant during the

PETM time interval. To create a quantitative age model from these concentrations the absolute flux of $^3He_{ET}$ to the sea floor during the PETM is needed. For this purpose, the $^3He_{ET}$ concentration of 13 samples taken from C24r and C25n were used to calculate the background flux of $^3He_{ET}$, adapting average sedimentation rates during these intervals from Aubry et al. (1996). Aubry et al. (1996) calculated these sedimentation rates based on the relatively poorly constrained magnetostratigraphy of Spiess (Spiess, 1990) - since then revised by Ali et al. (2000)- and durations for C24r and C25n of 2.557 and 1.650 myr (Cande and Kent, 1995), respectively. These sedimentation rates, however, are subject to several important problems: 1) the depth of the reversal between C24r and C24n has not been positively identified at Site 690, but nonetheless is used to calculate sedimentation rates. Recently it has been shown, however, that the carbon isotope excursion associated with Eocene thermal maximum 2 (ETM2), which is located ~180kyr before this magnetic reversal, is present at Site 690 (Chapter 2), and this depth can be used as a calibration point; 2) As mentioned above, the duration of Chron C24r was in the order of 3.118myr (Westerhold et al., submitted), which is 561 kyr longer than assumed in the $^3He_{ET}$ model; 3) ODP Site 690 recovered the early Paleogene in a single hole only. From multiple-hole drilling techniques, it has become clear that sediment cores expand when they are released from the overlying sediment and water column load, and thereby lose part of the core. For instance, the average expansion factor for the recently drilled Sites 1262-1267 at Walvis Ridge varied between 111 and 118% (Zachos et al., 2004), which implies recovery gaps of 1 to 1.8m between each core. With multiple-hole drilling, the composite depth scale is generated based on shipboard measurements, using the expanded cores. For this reason, sample depths relative to the composite depth scale become larger than in the meters below sea floor scale. Similarly, approximately 11 to 18% of the early Paleogene sediment section was likely lost during core recovery at Site 690. This aspect has not been accounted for by previous studies at Site 690, but obviously affects cycle counts (Norris and Röhl, 1999; Cramer et al., 2003) and sedimentation rates (Aubry et al., 1996; Farley and Eltgroth, 2003) over successive cores. Note, however, that the whole CIE is within one core at Site 690, so it did not affect the cycle count of Röhl et al. (2000) across the CIE.

Along with the uncertainties in the average sedimentation rates, the values of the 13 samples used to calculate the background $^3He_{ET}$ flux are likely affected by temporal (possibly orbitally-forced) variations in sedimentation rates. Hence, the actual $^3He_{ET}$ flux during the PETM may differ significantly from the average of the C24r-C25n interval. This uncertainty has likely been covered by the 'minimum' and 'maximum' estimates presented by Farley and Eltgroth that are based on the standard errors in the background flux values, which vary between 0.38 and 0.97pcc.cm^{-2}.kyr^{-1} (1 pcc = 10^{-12} cm^3 of He at STP). Moreover, as Farley and Eltgroth indicate, it is likely that the $^3He_{ET}$ fluxes were not constant during C24r

and C25n as this number may vary by an order of magnitude over millions of years (Farley, 2001). This is potentially reflected in the background flux values (see Background Data Set in (Farley and Eltgroth, 2003), which are significantly higher during C24r than during C25. However, the estimates of Farley & Eltgroth and cycle counting (Röhl et al., 2000) were very similar for the body of the CIE.

We try to correct for the above issues and assess the sensitivity of the $^3He_{ET}$ model for these uncertainties (Table 1). We adopt the durations of C25n (504kyr) and the interval between the onset of C24r and the ETM2 (2940kyr) from Westerhold et al. (submitted) and assess the sensitivity of the sedimentation rates to an 11% (i.e. lower estimate) core loss due to the expansion. Average values and standard deviations for the background $^3He_{ET}$ content/g sediment from Farley and Eltgroth (2003; Table 1c) are used to calculate absolute background fluxes through these intervals by excluding (Table 1a) and including (Table 1b) sediment expansion.

Farley and Eltgroth (2003) use a background flux of 0.69 ± 0.11 pcc.cm^{-2}.kyr^{-1}. The values in Table 1 indicate that the background flux during C25n was much lower than during C24r, suggesting that fluxes actually changed during this time interval. These values are averages of many individual measurements, which is likely to increase the reproducibility (Farley and Eltgroth, 2003). However, the standard deviations in the measurements are quite large (Table 1c), which may suggest that detectable variations in $^3He_{ET}$ flux occur even within these chrons. Further, the revised chron durations and the sediment expansion factor change the background flux estimates significantly. We have calculated several age models for the PETM using the various flux estimates (c.f., Farley and Eltgroth, 2003). The resulting profiles (shape and duration) of the CIE, using the bulk $\delta^{13}C$ curve of Bains et al., (1999), are plotted in Figure 3. It appears that the estimated duration of the CIE strongly depends on the expansion factor; the larger the expansion factor, the shorter the duration of the PETM (Figure 3). Applying the 11% expansion factor and a background flux based on all samples from C25n and C24r gives a CIE of 90–140kyr (Fig. 3C). But still this estimate includes many assumptions. For example, the absolute value of sediment expansion is an estimate from a different location. For our calculations we use a minimum estimate of 11%; an expansion of 18% would significantly shorten the duration of the PETM. Further, core recovery was not complete through the studied interval and the actual $^3He_{ET}$ flux during the PETM is likely to differ from any average. Generally, the sensitivity of the model to small changes in these assumptions is large.

In any case, the helium model invokes a very large increase in sedimentation rate towards the end of the PETM, which causes a rapid recovery period relative to the body of the PETM (Fig. 3; Farley and Eltgroth, 2003). This is potentially supported – although not known to which extent – by increased calcite production

a

Background ET3He flux and sedimentation rate model for Hole 690B. Expansion not included						
model (Fig. 5)	interval	duration (kyr)	thickness (cm)	sed rates (cm/kyr)		
I	C25n	504	937	1.86		cm/kyr
				dens/(kyr/cm)=	2.48	g/kyr
				av flux	**0.63**	pcc/cm2/kyr
				minus stand dev	**0.47**	pcc/cm2/kyr
				plus stand dev	**0.79**	pcc/cm2/kyr
II	base 24r - ETM 2	2940	5181	1.76		cm/kyr
				dens/(kyr/cm)=	2.35	g/kyr
				av flux	**0.79**	pcc/cm2/kyr
				minus stand dev	**0.71**	pcc/cm2/kyr
				plus stand dev	**0.87**	pcc/cm2/kyr
III	C25n - ETM 2	3444	6118	1.78		cm/kyr
				dens/(kyr/cm)=	2.37	g/kyr
				av flux	**0.71**	pcc/cm2/kyr
				minus stand dev	**0.56**	
				plus stand dev	**0.86**	

b

Background ET3He flux and sedimentation rate model for Hole 690B. Expansion (11%) included						
	interval	duration (kyr)	thickness (cm)	sed rates (cm/kyr)		
IV	C25n	504	1003	1.99		cm/kyr
				dens/(kyr/cm)=	2.66	g/kyr
				av flux	**0.68**	pcc/cm2/kyr
				minus stand dev	**0.51**	pcc/cm2/kyr
				plus stand dev	**0.85**	pcc/cm2/kyr
V	base 24r - ETM 2	3150	5809	1.84		cm/kyr
				dens/(kyr/cm)=	2.46	g/kyr
				av flux	**0.82**	pcc/cm2/kyr
				minus stand dev	**0.74**	pcc/cm2/kyr
				plus stand dev	**0.91**	pcc/cm2/kyr
VI	C25n - ETM 2	3654	6812	1.86		cm/kyr
				dens/(kyr/cm)=	2.49	g/kyr
				av flux	**0.74**	pcc/cm2/kyr
				minus stand dev	**0.58**	pcc/cm2/kyr
				plus stand dev	**0.90**	pcc/cm2/kyr

c

Background flux measurements	
Chron 24r	**Chron 25n+r**
ET3He pcc/g	ET3He pcc/g
0.28	0.30
0.35	0.23
0.35	0.19
0.31	0.36
0.39	0.21
0.33	0.24
0.33	**av 0.25**
av 0.33	**stdev 0.06**
stdev 0.03	
Chron 25 - ETM2 (all samples)	
ET3He pcc/g	
av 0.30	
stdev 0.06	
DB Density 1.34	

Table 1. Calculation of sedimentation rates and $^{3}He_{ET}$ fluxes through the upper Paleocene – lower Eocene section of ODP Hole 690B. Average values and standard deviations for the background $^{3}He_{ET}$ content/g sediment (from Farley and Eltgroth, 2003) in Table 1c are used to calculate absolute background $^{3}He_{ET}$ fluxes through the following intervals: onset – termination C25n, onset C24r – ETM2 and onset C25n – ETM2. For these calculations we adopt the durations of these intervals from Westerhold et al. (submitted) and exclude (Table 1a) and include (Table 1b) sediment expansion (see text).

in the photic zone (Kelly et al., 2005) or increased calcite preservation due to the 'overshoot' of the lysocline (see below; Chapter 1). Particularly in this aspect the helium model differs from the cycle model of Röhl et al., (2000), who counted 5-6 cycles through this interval. A cyclostratigraphic study on an Italian PETM section (Giusberti et al., submitted) also implied 5 precession cycles associated

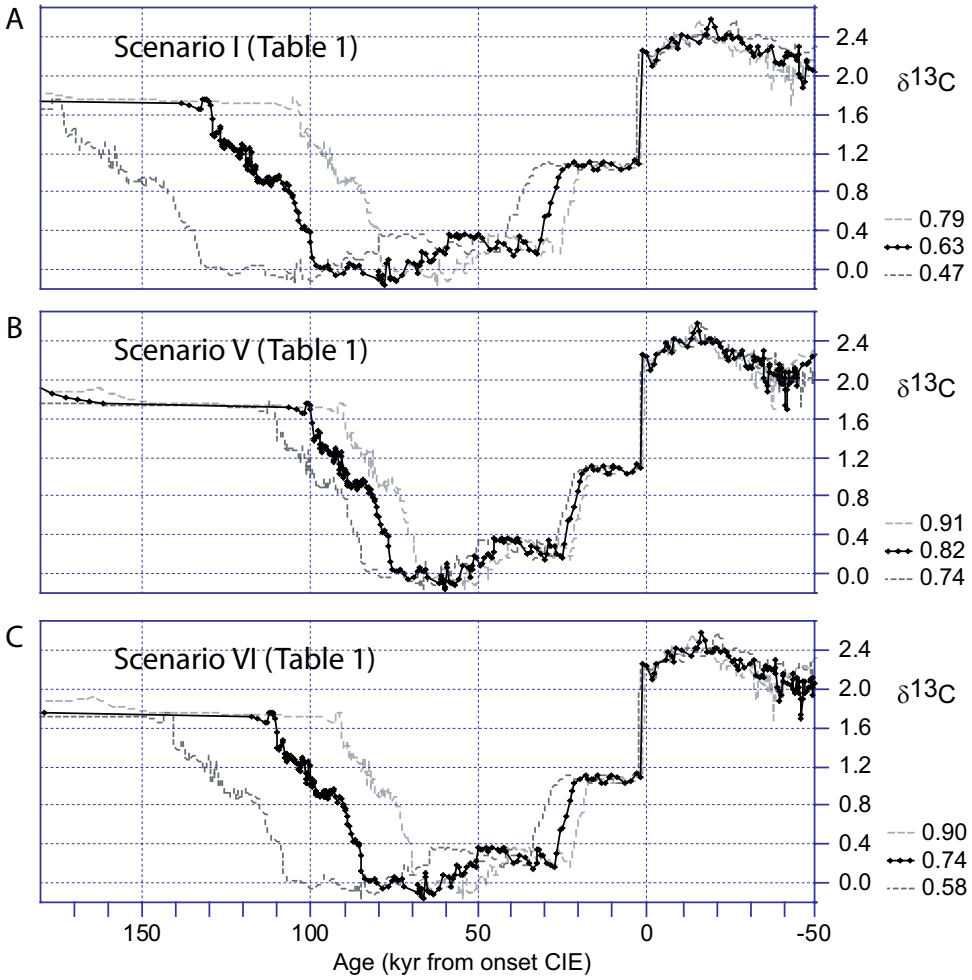

Figure 3. Shape and duration of the CIE (data from Bains et al., 1999) assuming the various options and uncertainties in sedimentation rates and background $^{3}He_{ET}$ fluxes calculated in Table 1. Options A, B and C represent scenarios I, V and VI from Table 1: **A.** $^{3}He_{ET}$ fluxes calculated from the measurements of C25 only (Table 1c) and sediment expansion not included, **B.** $^{3}He_{ET}$ fluxes calculated from the measurements of C24r and sediment expansion included, **C.** $^{3}He_{ET}$ fluxes calculated from the measurements of C25n through C24r and sediment expansion included. Dotted lines represent standard deviations of background flux measurements.

with the recovery interval, which would support the Röhl et al. model. However, direct correlation between this Italian section and Site 690 is hampered by the lack of a clear $\delta^{13}C$ inflection point at the termination of the CIE. Hence, although in general the helium model produces realistic estimates, it must be reproduced in multiple complete sections to tackle above discrepancies and uncertainties in the assumptions.

The temperature anomaly

Warming associated with the PETM has been shown in marine and terrestrial basins around the world and using various techniques. Deep sea benthic foraminiferal calcite consistently shows a >1‰ negative excursion in $\delta^{18}O$ (e.g., Kennett and Stott, 1991; Bralower et al., 1995; Thomas and Shackleton, 1996). Application of the empirical temperature-$\delta^{18}O$ relationship (e.g., Shackleton, 1967) indicates a deepwater temperature increase of ~4-5°C. This magnitude of warming is corroborated by benthic foraminifer Mg/Ca ratios (Tripati and Elderfield, 2005). At first, the negative $\delta^{18}O$ excursion in benthic foraminifera from the deep ocean was first interpreted as a shift from deep water formation at high latitudes to low latitudes (Kennett and Stott, 1991). Since then, accumulating evidence indicated that the dominant source of intermediate and deep water formation likely remained the high latitudes (Pak and Miller, 1992; Bice and Marotzke, 2001; Thomas, 2004). Regardless whether they derived from northern or southern high latitudes, the ~5°C warming of the intermediate or deep waters implies a ~5°C warming in subpolar regions (Tripati and Elderfield, 2005). Also planktonic foraminiferal $\delta^{18}O$ and Mg/Ca excursions generally point towards ~5°C warming (Kennett and Stott, 1991; Thomas and Shackleton, 1996; Charisi and Schmitz, 1998; Thomas et al., 2002; Zachos et al., 2003; Tripati and Elderfield, 2004), although at Site 690 the warming of surface waters appears to be as much as 6-8°C (Kennett and Stott, 1991; Thomas et al., 2002). Neritic benthic foraminifers locally show a larger $\delta^{18}O$ excursion (Cramer et al., 1999), locally supported by the organic paleothermometer TEX_{86}' (Chapters 4, 7), evidencing some spatial variation in temperature response.

Estimates from the terrestrial realm, dominantly from the Big Horn Basin in Wyoming, United States, are also in the range of 5°C. Koch et al (2003) and Bowen et al. (2001) calculate a 3-7°C warming based on carbonate soil nodule $\delta^{18}O$. Fricke and colleagues (Fricke et al., 1998; Fricke and Wing, 2004) infer that PETM mean annual temperature was 4-6°C warmer than during the uppermost Paleocene and the early Eocene, based on $\delta^{18}O$ of biogenic phosphate. Further, Wing et al. (2005) conclude a ~5°C rise in mean annual temperature during the PETM based on leaf margin analyses on macroscopic plant fossils.

A TEX_{86}' record across a PETM succession from the Arctic Ocean revealed a warming of ~5°C close to the North Pole (Chapter 3). Hence, the magnitude

of tropical and subpolar surface temperature changes was similar, suggesting that the PETM warming was not amplified at northern high latitudes (Tripati and Elderfield, 2005; Chapter 3). The absolute temperatures indicated by TEX_{86}' in the Arctic Ocean imply the absence of ice and thus exclude the influence of ice-albedo feedbacks on Arctic warming (Chapter 3), which likely accounts for the lack of polar amplification on the northern hemisphere.

Acidification of the ocean

According to theory, and as observed and expected in the present and future ocean (Caldeira and Wickett, 2003; Feely et al., 2004; Delille et al., 2005; Orr et al., 2005), the instantaneous induction of large amounts of CO_2 or CH_4 (which would rapidly be oxidized to CO_2 in the atmosphere) into the ocean-atmosphere system at the PETM should have increased the carbonic acid (H_2CO_3) concentration, leading to calcium carbonate dissolution (Dickens et al., 1997; Dickens, 2000). As a consequence, the extent of calcite compensation depth (CCD) shoaling is an indicator of the amount of CO_2 that was injected into the ocean-atmosphere system, and of the potential source of the carbon. Partial neutralization of excess CO_2 by increased carbonate dissolution has recently been well documented in sedimens across a ~2km depth transect (paleodepths ~ 1500-3600 m) at the Walvis Ridge (Chapter 1). But the dramatic shallowing of the CCD was not worldwide. Carbonate content at Site 690 (paleodepth ~ 1900 m), only decreases from ~85% to ~60%, a decrease that may not even have resulted from dissolution only (e.g., Bralower et al., 2004). The Mead Stream section in New Zealand located on the continental slope, does show a decreased carbonate content at the PETM, but this is interpreted as a higher terrestrial influx rather than dissolution (Hollis et al., 2005). The ~10% decrease in carbonate content at the central Pacific Site 1209 on the Shatsky Rise, which was also supposedly deeper than the shallowest Walvis Ridge site, appears minor (Colosimo et al., 2005). Although processes such as increased carbonate production and minor contribution of terrestrial material could be proposed to account for the seemingly high carbonate content at those sites, the behaviour of the CCD and lysocline and seafloor carbonate dissolution was not uniform across the ocean at the PETM. For example, dissolution has been observed at many, including marginal sites, such as the North Sea region (e.g., Gradstein et al., 1994), and the Tethys (e.g., Ortiz, 1995; Speijer and Wagner, 2002; Ernst et al., 2006). This heterogeneous response has, to date, impeded straightforward calculations of the absolute amount of carbon that was injected into the system at the onset of the CIE.

The recovery of the oceanic carbonate system has been attributed to the silicate weathering feedback, which has likely contributed to carbon sequestration during the recovery period (Chapter 1). This feedback, in combination with carbonate dissolution, likely caused the ocean to be extremely saturated with respect to carbonate ion, causing a gradual descent of the lysocline and CCD. It has been

shown that this oversaturation caused a descend of the lysocline to below the pre-PETM levels (Chapter 1). This aspect, and potentially higher surface productivity, likely caused the at least locally increased carbonate sedimentation during the recovery phase of the PETM (Kelly et al., 2005).

The role for organic carbon burial as potential mechanism to explain the gradual reduction in atmospheric CO_2 concentrations during the recovery phase has been explored in the deep marine and terrestrial realms (Bains et al., 2000; Beerling, 2000). Deep marine black shales, however, have not been recorded at the PETM, but expanded organic rich shallow marine successions are known from the Tethyan margins (e.g., Bolle et al., 2000; Speijer and Wagner, 2002; Gavrilov et al., 2003), the North Sea (e.g., Bujak and Brinkhuis, 1998) and the Arctic Ocean (Chapter 3). The amount of carbon buried in these deposits has not been estimated but appears very large, potentially invoking an important role for organic carbon burial during the sequestration of the excess carbon.

Biotic Response

The PETM is marked by extinctions, radiations, and migrations of species. Here, we summarize some of the main biotic responses in the benthic, pelagic as well as the terrestrial realms.

Patterns of benthic turnover

The PETM stands out in the geological record as one of the largest extinctions in deep marine calcareous benthic foraminifera, when 35-50% of the deep-sea species rapidly became extinct (Thomas, 1989; Pak and Miller, 1992; Thomas and Shackleton, 1996; Thomas, 1998; Thomas, 2003). Benthic foraminifer extinction (BFE) events of this magnitude are rare in the geological record and species turnover usually take place gradually over millions of years (Thomas, in press). Discussion on the cause of the extinction has concentrated on bottom water food availability, acidification, oxygen depletion and temperature. Such hypotheses are based on the paleoecological interpretations of post-BFE assemblages, which are unfortunately not straightforward (Thomas, 1998; Thomas, 2003). In terms of food availability, which usually depends on surface ocean production and export production of organic matter, deep sea benthic foraminifer assemblages have a geographically heterogeneous signature. In the central Pacific (ODP Site 865) and Southernmost Atlantic Ocean (Site 690), benthic foraminifer assemblages point to an increase in food supply, whereas the opposite is found at other Atlantic and Indian Ocean sites (Thomas, 2003). With higher temperatures, the food requirement of benthic foraminifers increases significantly because of higher metabolic rates, so there is no simple correlation between export productivity and apparent food supply to the benthic faunas. Nannofossil assemblages (see below) suggest a decrease in surface productivity at Sites 690 and 865, whereas benthic foraminiferal assemblages suggest an increased food

supply to the sea-floor. To explain this discrepancy, Thomas (2003) suggested that during the PETM either export production was more efficient, there was a food source at the ocean floor, or oxygen levels were lower resulting in lower organic matter decomposition. If the latter is true, decreased oxygen concentrations of the deep ocean due to higher temperatures and possibly methane oxidation (see below) may also have contributed to the BFE (Thomas, 1998; Dickens, 2000; Thomas, 2003). Nevertheless, deep marine black shales are not recorded from the PETM, there is no geochemical or sedimentological evidence for low oxygen conditions and the benthic foraminiferal assemblages do not support such a scenario (Thomas, in press). It appears likely that the occurrence of small and thin-walled benthic foraminifers (as well as ostracodes; Steineck and Thomas, 1996) in the interval just above the BFE, is associated with the increased calcite corrosiveness of the deep waters, or reflects a disturbed ecosystem (Thomas, 1998; Chapter 1). But minor extinctions occurred also among deep marine agglutinated foraminifera (Kaminski et al., 1996; Galeotti et al., 2005), which do not use calcite. Hence, temperature increase resulting in higher metabolic rates and higher food requirement, is currently thought to be the most important factor causing the BFE (Thomas, in press).

Benthic foraminifer studies on neritic and upper bathyal assemblages are largely restricted to the Tethyan basin and the Atlantic margins. These studies indicate that extinction and temporal changes in composition in these settings were less severe than in the deep sea (Speijer and Schmitz, 1998; Thomas, 1998; Cramer et al., 1999; Speijer and Wagner, 2002). Speijer and colleagues argue that late Paleocene through early Eocene assemblages generally indicate relatively oligotrophic conditions along the southern Tethyan margin, but show a transient increase in food supply during the PETM (Speijer and Schmitz, 1998; Speijer and Wagner, 2002; Scheibner et al., 2005). This interpretation is consistent with multi-proxy evidence from neritic realms around the world (see sections on dinocysts and nannofossils).

Unlike benthic foraminifera, the PETM does not stand out as a major extinction event in the deep sea ostracode fossil record, which, however, has not been well studied at high resolution. The only reasonable-resolution record from the deep sea is the one by Steineck and Thomas (1996) on assemblages from Site 689, which is close to Site 690. Their results indicate that ostracodes were smaller and thinner walled during the PETM, suggesting that within-lineage changes in ostracode morphology may reflect the same calcite corrosivity mechanism that may have forced widespread extinctions among benthic foraminifera.

Tethyan neritic ostracode assemblages on the other hand, do show a turnover at the PETM (Speijer and Morsi, 2002, and references therein), when long-ranging Paleocene taxa were outcompeted by a species that is thought to thrive in upwelling areas. Hence, the dominance of this species is interpreted as a response to enhanced

food supply and decreased bottom water oxygenation (Speijer and Morsi, 2002). Further, these Tethyan assemblages suggest a sea level rise at the PETM, an interpretation consistent with information from other shallow marine successions (Powell et al., 1996; Cramer et al., 1999; Crouch and Brinkhuis, 2005; Chapters 3 and 6).

Migration and radiation patterns in the planktonic realm

The most dramatic planktonic microfossil signature at the PETM is recorded in organic-walled dinoflagellate cysts (dinocysts). Organic cyst-forming dinoflagellates have life stratigies commonly involving neritic settings and are adapted to specific surface water conditions. They are very sensitive to changes in the physiochemical charateristics of the surface waters, which is reflected by their cysts in the sediment records. The taxon *Apectodinium* originated close to the Danian-Selandian boundary (Brinkhuis et al., 1994; Guasti et al., 2005) and abundant occurrences remained largely restricted to low latitudes throughout the Paleocene (Bujak and Brinkhuis, 1998). In contrast, every studied succession across the PETM that bears dinocysts yields abundant *Apectodinium*, usually >40% of the dinocyst assemblage (Heilmann-Clausen, 1985; Bujak and Brinkhuis, 1998; Heilmann-Clausen and Egger, 2000; Crouch et al., 2001; Chapters 3 and 7; Appendix 1 and references therein) (Fig. 4). Such a global, synchronous acme is unique in the dinocyst record, which indicates the extraordinary character of this event. Global warming at the PETM is likely to have warmed temperate to polar sea surface temperatures to allow poleward migration of *Apectodinium* (Bujak and Brinkhuis, 1998; Crouch et al., 2001). The *Apectodinium* acme appears, along with globally high sea-surface temperatures, associated with a strong increase in nutrient availability in marginal marine settings (Powell et al., 1996; Crouch et al., 2001; Crouch et al., 2003a; Crouch and Brinkhuis, 2005). The latter view is based on the concept that the motile dinoflagellates that formed *Apectodinium* cysts were likely heterotrophic and fed on organic detritus or other plankton that occurred in high abundances in marginal marine settings during this time interval (Bujak and Brinkhuis, 1998). Increased nutrient input by rivers to marginal marine settings is consistent with results from fully coupled general circulation models that predict an intensified hydrological cycle with elevated greenhouse gas concentrations (Pierrehumbert, 2002; Huber et al., 2003; Caballero and Langen, 2005). Further, other microfossil, clay mineralgeochemical and lithological evidence at least supports locally intensified runoff during the PETM (Robert and Kennett, 1994; Gibson et al., 2000; Ravizza et al., 2001; Speijer and Wagner, 2002; Egger et al., 2003; Gavrilov et al., 2003; Gibbs et al., 2006; Pagani et al., 2006). Along with thermophillic and heterotrophic, *Apectodinium* was likely euryhaline, i.e., tolerant to a wide range of salinities, as the acme has been recorded from the relatively fresh (Pagani et al., 2006; Chapter 3) Arctic Ocean to the likely more salty subtropical regions and even open ocean settings (Egger et al., 2000).

Because of their life strategy, marine dinoflagellate assemblages usually show a strong proximal-distal signal. Hence, the dinocyst assemblages from the sediments can be used to reconstruct the influence of inshore waters in a more offshore locality (Brinkhuis, 1994; Pross and Brinkhuis, 2005) Appendix 1). Globally, dinocyst assemblages show a trend towards more offshore surface water

Figure 3. Paleogeographic reconstruction of the earth during PETM times (modified from (Scotese, 2002) with the distribution of the dinocyst *Apectodinium*. All studied PETM sections that bear dinocysts yield abundant *Apectodinium*. Records are from the North Sea (Bujak and Brinkhuis, 1998, and references therein; Steurbaut et al., 2003), Greenland, Spitsbergen (e.g., Boulter and Manum, 1989; Nohr-Hansen, 2003), the Tethyan Ocean (N. Africa, Austria, Tunisia, Uzbekistan, Pakistan, India, Kazakhstan, e.g., Bujak and Brinkhuis, 1998; Crouch et al., 2003a; Iakovleva et al., 2001; Köthe et al., 1988), equatorial Africa (JanDuChêne and Adediran, 1984), the eastern (e.g. Edwards, 1989; Chapters 4 and 7) and north-western U.S. (J. Lucas-Clark, pers. comm., 2003), Barents Sea, South America (Brinkhuis, pers. obs.) and New Zealand (Crouch and Brinkhuis, 2005; Crouch et al., 2003b; Crouch et al., 2001) and the Arctic Ocean (Chapter 3).

conditions during the PETM (Crouch and Brinkhuis, 2005; Chapter 6; Appendix 1), implying that transgression took place at the PETM. Although the magnitude of this transgression is unclear, this transgression is consistent with data on shallow marine benthic foraminifer, ostracode and grain size information (Gibson and Bybell, 1994; Cramer et al., 1999; Speijer and Wagner, 2002; Speijer and Morsi, 2002).

Apectodinium was not only globally abundant at the PETM, this genus shows a large variation of morphotypes through this event. As for planktonic foraminifera (see below) it is hard to assess which of these dinocyst types represent true biological species. However, intermediate forms have been recorded between many of these morphotypes, implying that these represent ecophenotypes. On a higher taxonomic level, *Apectodinium* is member of the family Wetzeliellaceae, which underwent major radiation during or close to the PETM. Although high-resolution late Paleocene studies are rare (Brinkhuis et al., 1994; Iakovleva et al., 2001; Guasti et al., 2005), associated genera, such as *Wilsonidium*, *Dracodinium* and *Rhombodinium* originated close to or at the PETM. After the PETM, new genera and species within the Wetzeliellaceae, including the genus *Wetzeliella*, developed, potentially related to other early Eocene global warming events such as ETM2 (Chapter 2) and ETM3 (Röhl et al., 2006).

Compared to dinocysts, planktonic foraminifera show a relatively minor response to the PETM. Poleward migrations include the only occurrence of the low latitude genus Morozovella in the Weddel Sea (Thomas and Shackleton, 1996) just prior to and during the lower part of the CIE. Extinctions and radiations are largely absent but evidence of local faunal turnover has been recorded (e.g., Lu and Keller, 1993). The genera *Morozovella* and *Acarinina* developed extreme morphotypes during the PETM in tropical regions (Kelly et al., 1996; Kelly et al., 1998). The dominance of these newly developed taxa within the assemblages has been interpreted as indicative of relatively oligotrophic conditions in the open ocean due to changes in the thermal structure of the water column (Kelly et al., 1996). These PETM morphotypes might represent true evolutionary transitions or ecophenotypes reflecting unusual environmental conditions (Kelly et al., 1998).

Not many high-resolution calcareous nannofossil studies through the PETM have been focused on paleoecology, although assemblage changes are extensively described (e.g., Aubry et al., 1996; Raffi et al., 2005, and references therein). Bralower (2002) argued that nannofossil assemblages at Site 690 imply a change from abundant r-mode (in this case comprizing opportunistic species, indicating eutrophic conditions with a well-mixed upper water column and a shallow thermocline) to abundant k-mode (specialized species, indicating oligotrophic conditions with a stratified water column and a deep thermocline) species at the onset of the CIE. This interpretation is consistent with that of nannofossil

assemblage studies from the Indian Ocean (Tremolada and Bralower, 2004), the Pacific Ocean (Gibbs et al., 2006) and the Tethys (Monechi et al., 2000) and is supported by model studies (e.g., Boersma et al., 1998). Gibbs et al. (2006) describe neritic assemblages from the New Jersey shelf, and interprets these to reflect an increased productivity at the PETM.

In theory, a scenario of increased stratification in open ocean settings could well have resulted from surface warming (Huber et al., 2003). In contrast, increased accumulation of biogenic barite at the PETM at Site 690 and other sites has been ascribed to increased primary productivity (Bains et al., 2000). Dickens et al. (2003) suggested that hypothesized dissociation of methane hydrate at the PETM (see below) resulted not only in methane input, but also in Ba^{2+} release into the

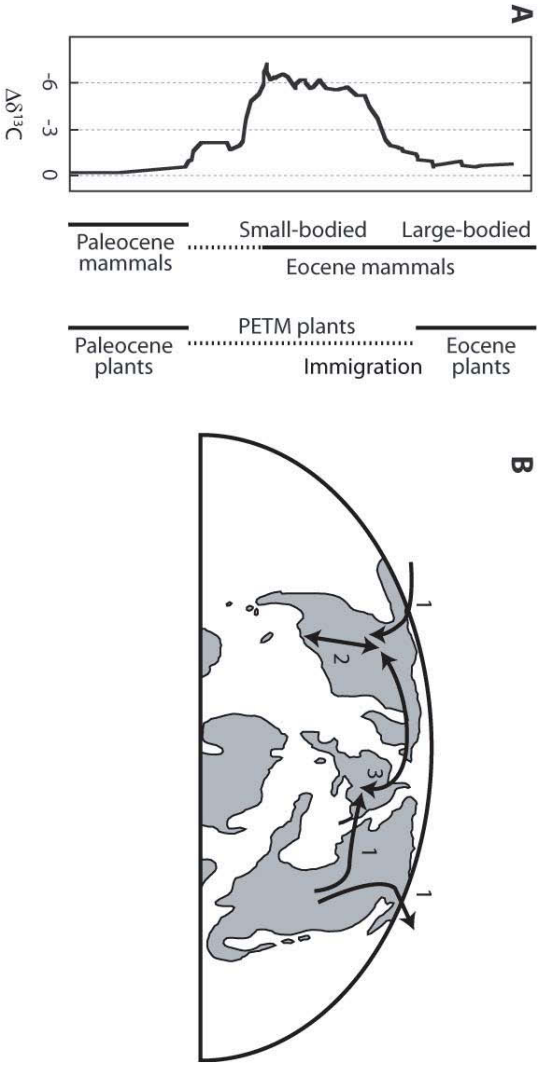

Figure 4. Patterns of terrestrial biotic change through the PETM. **A)** Temporal sequence of changes in mammal and plant assemblages, shown relative to the paleosol carbonate $\delta^{13}C$ curve for Polecat Bench, Wyoming, USA (carbon isotope values are shown here as anomalies relative to the average latest Paleocene values; after Bowen et al. (2006). **B)** Spatial pathways of migration thought to have been used by PETM intra- and inter-continental migrants. 1 - Directional exchange of mammals and turtles from Asia to North America and/or Europe. 2 - Northward range expansion of thermophillic plants from southern North America. 3 - Exchange of plant and mammal taxa between North America and Europe, including immigration of plant taxon to North America and homogenization of mammal faunas, including new PETM immigrants.

ocean, thus elevated dissolved Ba^{2+} concentrations in the deep sea, causing improved preservation of barite particlesIn addition, changes in bottom water CO_3^-, (described above) may have an effect on barite preservation (Schenau et al., 2001).

Terrestrial mammals

The PETM stands out as a time of significant changes in terrestrial biotic communities (Fig. 5). Perhaps the most dramatic, and certainly the best-known, of these is the abrupt introduction of 4 major taxonomic groups to terrestrial mammalian assemblages on the Northern-Hemisphere continents at or near the P-E boundary (Gervais, 1877; McKenna, 1983; Gingerich, 1989; Krause and Maas, 1990; Smith and Smith, 1995; Hooker, 1998). The first appearance of the ordinal-level ancestors of all modern hoofed mammals (orders Artiodactyla and Perissodactyla), the first Euprimates (those bearing the complete set of anatomical characteristics uniting modern primates), and a now-extinct family of carnivores (Hyaenodontidae) had long been held by paleontologists to represent the base of the Eocene in western North America and Europe (Gingerich and Clyde, 2001; Gingerich, 2006). Building on work begun in the early 1990s to constrain the timing of these first appearances relative to PETM climate change (Koch et al., 1992; Koch et al., 1995), recent high-resolution stratigraphic studies demonstrated they occur within meters of the CIE base at ~6 sites across the Holarctic continents (Cojan et al., 2000; Bowen et al., 2002; Steurbaut et al., 2003; Ting et al., 2003).

These first appearances initiated a profound modernization of mammal faunas that continued to be dominated by archaic forms despite prolific diversification following the Cretaceous-Paleogene boundary (Alroy et al., 2000). They are associated with both long- and short-term (transient) changes in terrestrial mammal faunas. In the context of longer-term changes in species diversity, the appearance event itself is overshadowed by rapid diversification within the new clades immediately following their introduction. This indicates that PETM-induced changes in terrestrial mammal faunas provided an evolutionary seed for groups that would come to be dominant components of Eocene to modern mammal faunas. Well-studied, high-resolution records from the northern Bighorn Basin of Wyoming also demonstrate that post-PETM assemblages have higher species richness, average species size, and proportional representation of herbivorous and frugiverous taxa than pre-PETM assemblages (Clyde and Gingerich, 1998) (Fig. 5). These changes reflect immediate impacts of addition of new species on mammalian community structure: changes that largely persisted and characterized early Eocene faunas of North America. Other of the impacts of the PETM on land mammals were transient, including a reduction in average individual body size in the Bighorn Basin, affecting both new PETM groups and lineages that ranged through the Paleocene-Eocene boundary (Gingerich, 1989; Clyde and

Gingerich, 1998) (Fig. 5). Body size in these lineages increased again immediately after the PETM. A significant taxonomic turnover between two groups of faunas assigned to the Bumbanian Asian land mammal age may also reflect a shift from transient PETM fauna to a more stable early Eocene fauna, and be somewhat analogous to North American faunal changes at the end of the PETM (Ting et al., 2003), although the data are at much lower resolution than those in the Bighorn Basin. No clear equivalent has been proposed for European faunas.

There is near-universal consensus that the abrupt first appearances in early Eocene mammal faunas represent synchronous dispersal of new taxa across Holarctica. Fossil biogeography (e.g., McKenna, 1983) and recent studies documenting Arctic Ocean paleo-salinity (Brinkhuis et al., 2006; Pagani et al., 2006; Chapter 3) suggest that the northern Hemisphere continents of the early Paleogene must have been linked at least intermittently by land bridges, which provided high-latitude corridors for faunal exchange among the continents. It has been inferred that warming of the continental climate during the PETM allowed mammals previously restricted to lower latitudes to access these inter-continental corridors, providing a trigger for the widespread dispersal of the new groups and homogenization of the Holarctic fauna (McKenna, 1983; Krause and Maas, 1990; Peters and Sloan, 2000).

This mechanism provides a compelling link between climate and PETM mammal turnover, but does not address the questions of where, when, or why the new immigrant groups originated. Two models for the origination of these groups have been proposed. Beard and colleagues have argued that the similarity between the early representatives of the new "PETM" groups and outgroup taxa from the Paleocene of Asia suggests an Asian origin of these clades during the Paleocene, and have further suggested that some primitive Asian representatives of the "new" clades may be of Paleocene age (Beard, 1998; Beard and Dawson, 1999). In contrast, Gingerich has argued that rapid origination of these clades in response to environmental perturbations associated with the PETM is both possible and plausible (Gingerich, 2006).

This debate centers on the issue of where and when the missing links between the new PETM groups and their ancestors occurred, and as a result it has been difficult to test the two competing ideas. Because the hypothesis for Asian origination predicts the presence of the new mammal groups in the Paleocene of Asia, however, chronostratigraphic correlation of mammal faunas from the Northern Hemisphere continents can be used to test this model. This approach has been applied to demonstrate the presence of Hyaenodontidae in Asian Paleocene faunas based on a combination of chemo-, magneto-, and biostratigraphic data (Bowen et al., 2002; Ting et al., 2003; Meng et al., 2004; Bowen et al., 2005). Recent work by Smith and colleagues (2006) has also argued for a slightly earlier appearance (by ca. 10 - 25 kry) of Primates in Asia. However,

the failure to find ubiquitous support for the hypothesis of Asian origination during the Paleocene, and recent evidence against other potential loci of Paleocene origination as candidates for the source of the PETM immigrants (Clyde et al., 2003), has led to renewed interest in the idea that environmental change during the PETM may have actually spurred the evolution and origination of several important extant orders (Gingerich, 2006).

Terrestrial plants

Palynological and macrofloral remains from the latest Paleocene and earliest Eocene have revealed no evidence for net long-term taxonomic turnover or long-lasting major changes in community structure associated with the PETM (Jaramillo and Dilcher, 2000; Harrington and Kemp, 2001; Wing and Harrington, 2001; Collinson et al., 2003; Crouch et al., 2003b; Crouch and Visscher, 2003; Harrington, 2003; Wing et al., 2003; Harrington et al., 2004). These studies documented modest floral change across the P-E boundary, including the introduction of a small number of immigrant taxa (e.g., introduction of some European taxa to North America) and increases in the diversity of floras from the late Paleocene to the early Eocene. Changes in terrestrial floras across the P-E boundary may have in some cases been diachronous and, at the least, do not stand out as highly anomalous relative to background spatial and temporal taxonomic variation (Harrington et al., 2004).

Two recently discovered floras of distinctive composition, however, show that major transient changes in the taxonomic composition of floras occurred during the PETM in the Bighorn Basin (Wing et al., 2005). These changes include the immigration of thermophillic taxa previously known from the southern United States and from adjacent basins of the western United States and the first appearance, later within the PETM, of the European immigrant palynospecies *Platycarya platycaryoides*. Hence, many early Paleogene plant taxa underwent major geographic range shifts during the PETM, both within and between continents. This has been interpreted to be consistent with floral range shifts at the end of the Pleistocene in that it demonstrates the rapid and plastic reorganization of plant communities in response to climatic and environmental change (Overpeck et al., 1992; Jackson and Overpeck, 2000; Wing et al., 2005).

Summary

Overall, response of the various marine groups with a fossil record to the PETM was heterogeneous. Benthic foraminifera comprise the only group that underwent a significant extinction event at the PETM, which is potentially related to the increased temperature, although carbonate corrosivity may have played a minor role. Deep sea ostracode faunas may also reflect this increased corrosivity, and are smaller and thinner-walled through the PETM (as are the benthic

foraminifera) at one deep sea site, but the geographical extent of this aspect is unclear due to the absence of published studies. In the surface ocean, a global acme of the exotic dinocyst *Apectodinium* is recorded along the continental margins, which along with increased temperature, has been interpreted as an increase in trophic level of marginal seas. The latter interpretation has locally been supported by neritic lithological, ostracode, benthic foraminifer and nannofossil information. Trophic levels in the open ocean are still debated: planktoic foraminiferal and nannofossil assemblages suggest that relatively oligotrophic conditions existed during the PETM, whereas increased barite concentrations (at some sites) have been interpreted as elevated surface productivity. Benthic foraminifera suggest an increase in food supply to the sea floor at some open ocean locations, but not necessarily higher surface productivity. Further, both dinocysts and neritic ostracodes indicate that eustatic sea level rise occurred at the PETM. Finally, the extreme morphotypes recorded in several planktic protist microfossil groups that are restricted to the PETM are likely to represent ecophenotypes.

The terrestrial biotic record of the PETM provides a strong demonstration of the power of climate change to induce changes in the geographic distribution of terrestrial organisms. Migration appears to be the dominant mechanism of change within PETM terrestrial ecosystems, not only within the mammal and plant records, but also among early Paleogene turtle faunas (Holroyd et al., 2001). This shifting of geographic distributions introduced new and unique taxonomic assemblages to PETM terrestrial ecosystems, but these changes appear to have been accomplished mainly through addition or substitution of taxa without significant loss or modification of existing groups (the example of transient body-size reduction in North American mammals being an important exception). One of the striking aspects terrestrial biotic change through the PETM is the lack of evidence for a PETM extinction event within any of the groups studied. Neither changes in the climatic and environmental landscape nor interactions among native and immigrant taxa seem to have had immediate "negative" impacts on the status of existing faunal and floral groups. This suggests a surprising level of adaptability within terrestrial ecosystems, although many details of the conditions and timing of PETM terrestrial environmental and biotic change remain to be resolved.

Hypotheses on the cause of the PETM

Proxy data and model studies of the PETM unequivocally point towards the injection of large amounts of carbon into the ocean-atmosphere system, but the source of this carbon has not yet been elucidated. Hypothesis that have been and will be proposed should be consistent with the climatic and geochemical changes that characterize the PETM. Such hypotheses should explain a surface and deep water temperature increase of 5-6°C (Chapters 3, 4 and 7; Kennett and Stott, 1991; Koch et al., 1995; Thomas et al., 2002; Zachos et al., 2003; Tripati and

Elderfield, 2005) and a 3-5 ‰ negative carbon isotope excursion in the exogenic carbon pool (Kennett and Stott, 1991; Koch et al., 1992; Thomas et al., 2002; Pagani et al., 2006). Further, they should explain the widespread dissolution of carbonates in the deep marine realm (while keeping track of the geographic variability of the CCD response), which should be proportional to the amount of carbon injected into the system (Chapter 1) and the biotic changes that characterize the PETM. Critically, they must explain why similar events, such as ETM2 (Chapter 2) and ETM3 (Röhl et al., 2006) occurred millions of years after the PETM and why the onset of all these events appear to correlate to maxima in eccentricity (Chapter 2).

Because many proposed hypotheses cannot satisfy the latter constraint, we first focus on the study presented in Chapter 2. In theory, on a long-term gradual climate trend, temporal extremes are expected to occur during eccentricity maxima when seasonal contrasts on both hemispheres are maximized and critical climate thresholds are likely to be surpassed. The climate of the late Paleocene through early Eocene followed a clear long term warming trend, as evidenced by benthic foraminifer $\delta^{18}O$ (Zachos et al., 2001). This warming is potentially related to increasing CO_2 levels through high volcanic activity in the North Atlantic Igneous Province (Schmitz et al., 2004; Thomas and Bralower, 2005; Maclennan and Jones, 2006) and along Indian Ocean spreading zones (Cogné and Humler, 2006). The Late Paleocene is also characterized by a long-term decrease in benthic foraminifer (and likely global exogenic) $\delta^{13}C$ after the major positive event in mid paleocene (Zachos et al., 2001). The eccentricity maxima superimposed on these trends could have comprised thresholds for transient events and resulting climate change.

The spectral characteristics of magnetic susceptibility and colour reflectance records of continuous and complete lower Paleogene deep sea sedimentary successions from the Ocean Drilling Program Leg 208 on the Walvis Ridge reveiled that both the PETM and the ETM2 (Chapter 2) and ETM3 (Röhl et al., 2006) transient global greenhouse warming events set on during eccentricity maxima (Chapter 2). This may point towards an insolation-driven forcing mechanism for these events. Recently, Westerhold et al. (submitted) demonstrate however that a similar statistical treatment, but in this case on high-resolution Fe and a* records of the same Walvis Ridge sites, resulted in two short-term eccentricity cycles less between the PETM and ETM2 then found in Chapter 2. This most likely implies that both events do not exactly correspond with a maximum in the long-term (405kyr) eccentricity cycle, but depend on one of the short-term (100kyr) eccentricity extremes superimposed on these long-term cycles. A clue to this orbital-based forcing mechanism of the late Paleocene to early Eocene warming events may become soon available when a new generation of astronomical calculations will be launched (Laskar, pers. comm.).

An important consequence of the orbital-based forcing mechanism theory is that, unique events such as comet impacts (Kent et al., 2003; Cramer and Kent, 2005), which were already subject of intense debate (Dickens and Francis, 2003), explosive volcanism (Bralower et al., 1997; Schmitz et al., 2004), intrusion-forced injection of thermogenic methane (Svensen et al., 2004) and tectonic uplift-forced methane hydrate release (Maclennan and Jones, 2006) can be excluded. Similarly, dessication of epicontinental seas (Higgins and Schrag, 2006), an lithospheric gas explosions (Phipps Morgan et al., 2004), can be excluded even though some of these hypotheses seem appealing because they can explain other aspects of the PETM. Regardless of the potential astronomical pacing of the PETM, ETM2 and ETM3 events, the simple fact that multiple events occurred and that they are restricted to the late Paleocene and early Eocene increase the likeliness of a trigger on earth as a cause for these events.

In the present day situation, carbons reservoirs one earth that are capable of injecting the required amount of ^{13}C-depleted carbon required to generate the CIE in the atmosphere and ocean are scarce (Dickens et al., 1995; Dickens et al., 1997). The potential reservoir is methane hydrates, which has a $\delta^{13}C$ of ~-60‰, although the size of this reservoir is subject of discussion (Milkov, 2004). The methane that is incorporated into the hydrates is produced by anoxic bacterial decomposition or thermogenic breakdown of organic matter (Kvenvolden, 1988; Kvenvolden, 1993). In the present ocean, these hydrates are stable along continental slopes at relatively high pressure and low temperatures and can rapidly dissociate when pressure falls or temperature rises. During the much warmer latest Paleocene, hydrates were likely only stable at larger waterdepths, suggesting that the reservoir was smaller than at present. However, methane hydrates were potentially present at greater depths dan at present. This would have required that more organic matter was present further away from the continents than nowadays, perhaps in conjunction with lower oxygen content of the bottom waters resulting from higher temperatures.

The dissociation of methane clathrates along continental slopes has been invoked to explain the CIE and part of the climatic warming (Dickens et al., 1995; Matsumoto, 1995). Although the residence time of CH_4 increases during episodes of large emissions, CH_4 is oxidized to CO_2 within a century (Schmidt and Schindell, 2003), indicating that greenhouse warming from methane injection largely would result from CO_2 forcing. As already pointed out by Dickens et al. (1997), the radiative forcing of the excess CO_2 resulting from the injection of ~2,000 Gt of biogenic methane - required to generate the CIE (Dickens et al., 1995) - appears not enough to explain the magnitude of climate warming, indicating that additional warming mechanisms are required in this hypothesis (e.g., Dickens et al., 1997; Schmidt and Schindell, 2003; Archer, in press). Further, if the CIEs related to ETM2 and ETM3 were also caused by the dissociation of

methane hydrates, this requires a much faster replenishment of the reservoir in the early Eocene than known from present hydrates (Fehn et al., 2000), or that not all hydrates dissociated during the PETM and ETM2.

In their study to assess terrestrial and marine carbon burial rates, Kurtz et al. (2003) capitalize on the expected coupling between the carbon and sulphur cycles during marine organic carbon burial to show that much organic carbon was buried on the continents through the late Paleocene. These authors suggest that rapid oxidation (burning) of this terrestrial organic carbon, in their words "*global conflagration*", could have at least contributed to the CIE and climate warming. High concentrations of macroscopic charcoal have indeed locally been recorded at the PETM (Collinson et al., 2003), although these do not support a scenario of peat burning (Collinson et al., 2006). Because terrestrial organic matter (~-30‰) is much less ^{13}C-depleted than methane hydrates, much more carbon would in that case have entered the atmosphere and ocean to generate the CIE. Hence, due to the higher mass of carbon injected, the enhanced radiative forcing resulting from the burning of peat would be much larger than that resulting from the release of methane hydrates (Kurtz et al., 2003; Higgins and Schrag, 2006). However, it is not clear if the terrestrial organic carbon reservoir was large enough in the late Paleocene to account for the magnitude of the CIE, also because significant Upper Paleocene peat deposits are still found today. Although problems still exist for the latter two hypotheses, they are potentially climatically-induced and associated with orbital forcing. The thresholds to dissociate methane hydrates or burn buried terrestrial organic carbon possibly comprised increased intermediate water temperatures or drought in specific regions, respectively. To invoke such mechanisms as a cause of the PETM particularly requires good documentation of the character, trends and dynamics of Late Paleocene climate including its response to the orbital cycles, which is at present not available.